Classification of spherically symmetric self-similar dust models

B. J. Carr
Astronomy Unit, Queen Mary & Westfield College, Mile End Road, London E1 4NS, England
and Yukawa Institute for Theoretical Physics, Kyoto University, Kyoto 606-8502, Japan
(Received 23 December 1999; published 24 July 2000)

We classify all spherically symmetric dust solutions of Einstein's equations which are self-similar in the sense that all dimensionless variables depend only upon $z \equiv r/t$. We show that the equations can be reduced to a special case of the general perfect fluid models with an equation of state $p = \alpha\mu$. The most general dust solution can be written down explicitly and is described by two parameters. The first one (E) corresponds to the asymptotic energy at large $|z|$, while the second one (D) specifies the value of z at the singularity which characterizes such models. The $E = D = 0$ solution is just the flat Friedmann model. The 1-parameter family of solutions with $z > 0$ and $D = 0$ are inhomogeneous cosmological models which expand from a big bang singularity at $t = 0$ and are asymptotically Friedmann at large z; models with $E > 0$ are everywhere underdense relative to Friedmann and expand forever, while those with $E < 0$ are everywhere overdense and recollapse to a black hole containing another singularity. The black hole always has an apparent horizon but need not have an event horizon. The $D = 0$ solutions with $z < 0$ are just the time reverse of the $z > 0$ ones, having a big crunch at $t = 0$. The 2-parameter solutions with $D > 0$ again represent inhomogeneous cosmological models but the big bang singularity is at $z = -1/D$, the big crunch singularity is at $z = +1/D$, and any particular solution necessarily spans both $z < 0$ and $z > 0$. While there is no static model in the dust case, all these solutions are asymptotically ''quasi-static'' at large $|z|$. As in the $D = 0$ case, the ones with $E \geqslant 0$ expand or contract monotonically but the latter may now contain a naked singularity. The ones with $E < 0$ expand from or recollapse to a second singularity, the latter containing a black hole. The 2-parameter solutions with $D < 0$ models either collapse to a shell-crossing singularity and become unphysical or expand from such a state.

PACS number(s): 04.20.Jb, 95.30.Sf, 98.80.Hw

I. INTRODUCTION

Spherically symmetric self-similar solutions to Einstein's equations have the feature that every dimensionless variable is a function of some dimensionless combination of the cosmic time coordinate t and the comoving radial coordinate r. In the simplest situation, a self-similar solution is invariant under the transformation $r \rightarrow at, t \rightarrow at$ for any constant a, so the similarity variable is $z = r/t$. Geometrically this corresponds to the existence of a homothetic Killing vector. Such solutions have been the focus of much attention in general relativity because the field equations simplify to ordinary differential equations [1].

Even greater simplification is afforded if one focuses on the situation in which the source of the gravitational field is pressureless dust since, in this case, the solutions can often be expressed analytically and are just a special subclass of the more general spherically symmetric Tolman-Bondi solutions [2]. A number of people have studied such solutions [3–6] and these papers are described in some detail by Krasinski [7] and Carr and Coley [8]. Of particular physical interest has been the use of self-similar dust solutions in studying naked singularities [9] and modeling cosmic voids [10,11].

In this paper we will present a classification of spherically symmetric homothetic dust models which is ''complete'' subject to certain specified restrictions. This serves as a first step in the more general analysis, presented in an accompanying paper [12], of spherically symmetric self-similar perfect fluid models with pressure, the equation of state then necessarily being of the form $p = \alpha\mu$. Despite the simplifications entailed, we will find that many of the features of the $\alpha = 0$ (dust) solutions carry over to the $\alpha \neq 0$ case, at least in the supersonic regime. In particular, many (though not all) of the types of solutions with pressure have direct analogues in the dust case. Our aim is therefore to use the exact analytic dust solutions to derive qualitative features of self-similar solutions which will also turn out to pertain when there is pressure but which can then only be demonstrated numerically. On the other hand, it should be stressed that the introduction of pressure is also associated with many new features—especially in the subsonic regime—which cannot be understood in this way.

The plan of the paper is as follows: In Sec. II we will show how the dust equations can be regarded as a special case of the equations with pressure providing one adopts a specific prescription in taking the limit $\alpha \rightarrow 0$. In Sec. III we discuss the general family of dust self-similar solutions, showing that they can be conveniently categorized as asymptotically Friedmann and what we term asymptotically quasi-static. In each case, we will focus on the important physical features of the solutions, such as the presence of apparent horizons, event horizons and singularities. We will also clarify the connection between models with positive and negative z. We will specify the sense in which our classification is ''complete'' in Sec. IV.

II. SPHERICALLY SYMMETRIC SIMILARITY SOLUTIONS

In the spherically symmetric situation one can introduce a time coordinate t such that surfaces of constant t are orthogo-

nal to fluid flow lines and comoving coordinates (r,θ,ϕ) which are constant along each flow line. The metric can then be written in the form

$$ds^2=e^{2\nu}\,dt^2-e^{2\lambda}\,dr^2-R^2\,d\Omega^2,\quad d\Omega^2\equiv d\theta^2+\sin^2\theta\,d\phi^2 \tag{2.1}$$

where ν, λ and R are functions of r and t. The Einstein equations have a first integral

$$m(r)=\tfrac{1}{2}R\left[1+e^{-2\nu}\left(\frac{\partial R}{\partial t}\right)^2-e^{-2\lambda}\left(\frac{\partial R}{\partial r}\right)^2\right]. \tag{2.2}$$

This can be interpreted as the mass within comoving radius r at time t:

$$m(r)=4\pi\int_0^r \mu R^2\frac{\partial R}{\partial r'}\,dr' \tag{2.3}$$

where $\mu(r,t)$ is the energy density and we choose units in which $c=G=1$. This is constant if $p=0$. Equation (2.2) can be written as an equation for the energy per unit mass of the shell with comoving coordinate r:

$$\begin{aligned} E&\equiv\frac{1}{2}(\Gamma^2-1)=\frac{1}{2}U^2-\frac{m}{R},\\ U&\equiv e^{-\nu}\left(\frac{\partial R}{\partial t}\right),\quad \Gamma\equiv e^{-\lambda}\left(\frac{\partial R}{\partial r}\right). \end{aligned} \tag{2.4}$$

This can be interpreted as the sum of the kinetic and potential energies per unit mass. E and Γ are conserved along fluid flow lines in the $p=0$ case.

By a spherically symmetric similarity solution we shall mean one in which the spacetime admits a homothetic Killing vector $\boldsymbol{\xi}$ that satisfies

$$\xi_{\mu;\nu}+\xi_{\nu;\mu}=2g_{\mu\nu}. \tag{2.5}$$

This means that the solution is unchanged by a transformation of the form $t\to at$, $r\to ar$ for any constant a. Solutions of this sort were first investigated by Cahill and Taub [1], who showed that by a suitable coordinate transformation they can be put into a form in which all dimensionless quantities such as ν, λ, E and

$$S\equiv\frac{R}{r},\quad M\equiv\frac{m}{R},\quad P\equiv pR^2,\quad W\equiv\mu R^2 \tag{2.6}$$

are functions only of the dimensionless variable $z\equiv r/t$. This means that the field equations reduce to a set of ordinary differential equations in z. Another important quantity is the function

$$V(z)=e^{\lambda-\nu}z, \tag{2.7}$$

which represents the velocity of the surfaces of constant z relative to the fluid. These surfaces have the equation $r=zt$ and therefore represent a family of spheres moving through the fluid. The spheres contract relative to the fluid for $z<0$ and expand for $z>0$. This is to be distinguished from the velocity of the spheres of constant R relative to the fluid:

$$V_R=-\frac{U}{\Gamma}=-e^{\lambda-\nu}\left(\frac{\partial R/\partial t}{\partial R/\partial r}\right). \tag{2.8}$$

This is positive if the fluid is collapsing and negative if it is expanding. Special significance is attached to values of z for which $|V|=1$ and $|V_R|=1$. The first corresponds to a Cauchy horizon (either a black hole event horizon or a cosmological particle horizon) and the second to a black hole or cosmological apparent horizon. One can show [4] that the existence of an apparent horizon is also equivalent to the condition $M=1/2$.

Although our main focus in this paper is (pressureless) dust solutions, it is elucidating to start by considering the equations for a fluid with pressure. We will follow the formalism of Carr and Yahil [5]. The only barotropic equation of state compatible with the similarity ansatz is one of the form $p=\alpha\mu$ $(-1\leqslant\alpha\leqslant 1)$. If one introduces a dimensionless function $x(z)$ defined by

$$x(z)\equiv(4\pi\mu r^2)^{-\alpha/(1+\alpha)}, \tag{2.9}$$

then the conservation equations $T^{\mu\nu}{}_{;\nu}=0$ can be integrated to give

$$e^{\nu}=\beta x z^{2\alpha/(1+\alpha)} \tag{2.10}$$

$$e^{-\lambda}=\gamma x^{-1/\alpha}S^2 \tag{2.11}$$

where β and γ are integration constants. The remaining field equations reduce to a set of ordinary differential equations in x and S:

$$\ddot{S}+\dot{S}+\left(\frac{2}{1+\alpha}\frac{\dot{S}}{S}-\frac{1}{\alpha}\frac{\dot{x}}{x}\right)[S+(1+\alpha)\dot{S}]=0, \tag{2.12}$$

$$\left(\frac{2\alpha\gamma^2}{1+\alpha}\right)S^4+\frac{2}{\beta^2}\frac{\dot{S}}{S}x^{(2-2\alpha)/\alpha}z^{(2-2\alpha)/(1+\alpha)}-\gamma^2S^4\frac{\dot{x}}{x}\left(\frac{V^2}{\alpha}-1\right)$$
$$=(1+\alpha)x^{(1-\alpha)/\alpha}, \tag{2.13}$$

$$M=S^2x^{-(1+\alpha)/\alpha}\left[1+(1+\alpha)\frac{\dot{S}}{S}\right], \tag{2.14}$$

$$M=\frac{1}{2}+\frac{1}{2\beta^2}x^{-2}z^{2(1-\alpha)/(1+\alpha)}\dot{S}^2-\frac{1}{2}\gamma^2x^{-(2/\alpha)}S^6\left(1+\frac{\dot{S}}{S}\right)^2, \tag{2.15}$$

where the velocity function is given by

$$V=(\beta\gamma)^{-1}x^{(1-\alpha)/\alpha}S^{-2}z^{(1-\alpha)/(1+\alpha)} \tag{2.16}$$

and an overdot denotes $z\,d/dz$. The other velocity function is

$$V_R = \frac{V\dot{S}}{S+\dot{S}} \tag{2.17}$$

and, from Eqs. (2.4) and (2.15), the energy function is

$$E = \frac{1}{2}\gamma^2 x^{-(2/\alpha)} S^6 \left(1+\frac{\dot{S}}{S}\right)^2 - \frac{1}{2}, \tag{2.18}$$

which necessarily exceeds $-1/2$.

We can best envisage how these equations generate solutions by working in the 3-dimensional $(x,S,\dot{S})$ space [5]. At any point in this space, for a fixed value of α, Eqs. (2.14) and (2.15) give the value of z; Eq. (2.13) then gives the value of $\dot{x}$ unless $|V|=\sqrt{\alpha}$ and Eq. (2.12) gives the value of $\ddot{S}$. Thus the equations generate a vector field $(\dot{x},\dot{S},\ddot{S})$ and this specifies an integral curve at each point of the 3-dimensional space. Each curve is parametrized by z and represents one particular similarity solution. This shows that, for a given equation of state parameter α, there is a 2-parameter family of spherically symmetric self-similar solutions. In general there would be a sonic point, with possible associated discontinuities, at $|V|=\sqrt{\alpha}$. This corresponds to crossing a 2-dimensional surface in the solution space but we need not discuss this complication here.

Henceforth we focus on the dust solutions. Although Eqs. (2.10) to (2.16) break down when $\alpha=0$, in that some of the terms disappear or diverge, we will show that the equations are still formally applicable providing the function x defined by Eq. (2.9) is set to 1 whenever it does not appear with the exponent $1/\alpha$. Otherwise one must make the substitution

$$x^{1/\alpha} \to (4\pi\mu r^2)^{-1}, \quad \frac{1}{\alpha}\frac{\dot{x}}{x} \to -\frac{d\ln(\mu r^2)}{d\ln z}, \tag{2.19}$$

as suggested by Eq. (2.9). In fact, the relevant equations are most simply obtained by noting that both the energy and mass within comoving radius r are conserved, so that E and $m/r=MS$ are constant. If we put $m/r=\kappa$, then Eq. (2.3) implies

$$4\pi\mu R^2 \frac{\partial R}{\partial r} = \frac{dm}{dr} = \kappa \tag{2.20}$$

and this can be combined with Eqs. (2.9) and (2.11) to give

$$e^{\lambda} = \gamma^{-1}(4\pi\mu r^2 S^2)^{-1} = \kappa^{-1}\gamma^{-1}\frac{\partial R}{\partial r}. \tag{2.21}$$

On the other hand, Eq. (2.4) implies $e^{\lambda}=\Gamma^{-1}(\partial R/\partial r)$ where $\Gamma=\pm\sqrt{1+2E}$ and so the constant κ is just Γ/γ. The mass function is therefore

$$M = \frac{\Gamma}{\gamma S} = \frac{\sqrt{1+2E}}{\gamma S}, \tag{2.22}$$

where we have taken the positive square root for Γ to ensure that the mass if positive. (We discuss the negative mass case later.) Putting $x=1$ in Eq. (2.10) also gives $e^{\nu}=\beta$, so Eq. (2.4) can be rewritten as

$$E = \frac{1}{2\beta^2} z^4 \left[\frac{dS}{dz}\right]^2 - \frac{\sqrt{1+2E}}{\gamma S}. \tag{2.23}$$

Once this equation has been integrated to give $S(z)$, all the other functions can be obtained, so one has solved the problem completely.

We now show that Eqs. (2.10) to (2.16) are all formally satisfied if one uses the prescription given by Eq. (2.19). Equation (2.14) can be written as

$$MS = m/R = S^2(4\pi\mu r^2)(S+\dot{S}) = 4\pi\mu R^2 \frac{\partial R}{\partial r} \tag{2.24}$$

and this is just equivalent to Eq. (2.20). Since Eq. (2.21) implies

$$(4\pi\mu r^2)^{-1} = \gamma S^2 (S+\dot{S})/\Gamma, \tag{2.25}$$

we also have

$$\frac{d\ln(\mu r^2)}{d\ln z} = -\frac{2\dot{S}}{S} - \frac{\dot{S}+\ddot{S}}{S+\dot{S}}. \tag{2.26}$$

Equation (2.12) is then automatically satisfied and, from Eq. (2.23), formally corresponds to $\dot{E}=0$. Finally we can substitute for the x terms in Eq. (2.13), using Eqs. (2.19) and (2.25), to obtain

$$\ddot{S}+\dot{S} = -\frac{\Gamma}{S^2 z^2} \tag{2.27}$$

and this can be integrated to give Eq. (2.23).

It is now convenient to scale the r and t coordinates so that $\beta=\gamma=1$. Equation (2.23) then implies

$$\frac{dS}{dz} = \pm\frac{\sqrt{2E+2\Gamma/S}}{z^2} \tag{2.28}$$

and this can be integrated to give

$$D\mp\frac{1}{z}=\begin{cases}\dfrac{\sqrt{ES^2+\Gamma S}}{\sqrt{2}E}-\dfrac{2\Gamma}{(2E)^{3/2}}\sinh^{-1}\sqrt{\dfrac{ES}{\Gamma}} & (E>0),\\ \dfrac{\sqrt{2}}{3}S^{3/2} & (E=0),\\ \dfrac{2\Gamma}{(-2E)^{3/2}}\sin^{-1}\sqrt{\dfrac{-ES}{\Gamma}}\pm\dfrac{\sqrt{ES^2+\Gamma S}}{\sqrt{2}E} & (-1/2<E<0),\end{cases} \tag{2.29}$$

where D is an integration constant and $\sin^{-1}$ is taken to lie between 0 and π. In the first two cases, the upper and lower signs on the left-hand-side apply for dS/dz positive and negative, respectively, this sign being constant for any particular solution. In the third case, the sign on the left is fixed for a particular solution, even though dS/dz may switch sign, but the sign of the last term is plus if $\sin^{-1}$ lies between 0 and $\pi/2$ and minus if it lies between $\pi/2$ and π. If we took the negative square root in Eq. (2.22), corresponding to M and Γ being negative, there would be another solution for $E>0$ given by

$$D\mp\frac{1}{z}=\frac{\sqrt{ES^2-|\Gamma|S}}{\sqrt{2}E}+\frac{2|\Gamma|}{(2E)^{3/2}}\cosh^{-1}\sqrt{\frac{ES}{|\Gamma|}}\quad(E>0). \tag{2.30}$$

This solution is unphysical, since the mass is negative, but it is of interest for comparison with the solutions with pressure.

Equations (2.16), (2.17), (2.19), (2.25) and (2.28) give the velocity functions as

$$V=\frac{Sz\pm\sqrt{2E+2\Gamma/S}}{\Gamma} \tag{2.31}$$

and

$$V_R=\pm\frac{\sqrt{2E+2\Gamma/S}}{\Gamma}, \tag{2.32}$$

while Eqs. (2.16) and (2.31) imply that the density is given by

$$4\pi\mu t^2=\frac{1}{zS^2V}=\frac{\Gamma}{zS^2(Sz\pm\sqrt{2E+2\Gamma/S})}, \tag{2.33}$$

where the upper and lower signs again correspond to dS/dz being positive and negative, respectively. Note that V is negative (corresponding to tachyonic models) for the solution given by Eq. (2.30) and μ is also negative. In all cases the metric can be written as

$$ds^2=dt^2-\frac{(S+\dot{S})^2}{1+2E}dr^2-r^2S^2d\Omega^2, \tag{2.34}$$

which is the standard Tolman-Bondi form with constant energy function $E(r)$.

III. CLASSIFICATION OF SOLUTIONS

Equation (2.29) implies that there is a 2-parameter family of similarity solutions (as in the general α case). In this section we will provide a complete description of these solutions. We will start by considering the simplest one: the flat Friedmann solution with $D=E=0$. We will then consider the one-parameter family of solutions with $E\neq0$, $D=0$. Finally we will consider the full two-parameter family of solutions with $E\neq0$, $D\neq0$. In each case, we will show the form of the physically interesting quantities S, V and μt^2 as functions of z. In obtaining the full family of solutions, it is crucial that we allow z to be either positive or negative. Our analysis will also cover the (presumably unphysical) solutions with negative mass because they relate to some of the solutions with pressure.

A. $E=D=0$ solution

In this case Eqs. (2.29), (2.31) and (2.33) give

$$S=(\sqrt{2}z/3)^{-2/3}=M^{-1},\quad V=(z/6)^{1/3},\quad \mu=(6\pi t^2)^{-1}. \tag{3.1}$$

This corresponds to the standard dust Friedmann model with zero curvature constant. The metric can be put in the usual form by making the substitution $\hat{r}=(9r/2)^{1/3}$, which gives

$$ds^2=dt^2-t^{4/3}[d\hat{r}^2+\hat{r}^2d\Omega^2]. \tag{3.2}$$

Note that the curvature constant must be zero because otherwise there would be an intrinsic scale, which would contradict the similarity assumption.

B. $D=0$ solutions

Solutions with $D=0$ are asymptotically Friedmann as $|z|\to\infty$ and are specified entirely by the energy parameter E. These were originally studied by Carr and Hawking [4] and Carr and Yahil [5]. The form of $S(z)$ in these solutions is shown in Fig. 1(a), the arrows always corresponding to the direction of increasing time. The solutions with $z>0$ correspond to initially expanding big bang models: they start from a big bang singularity ($S=0$) at $t=0$ ($z=\infty$) and then either expand indefinitely ($S\to\infty$) as $t\to\infty$ ($z\to0$) for $E\geqslant0$ or recollapse to a black hole singularity ($S=0$) at

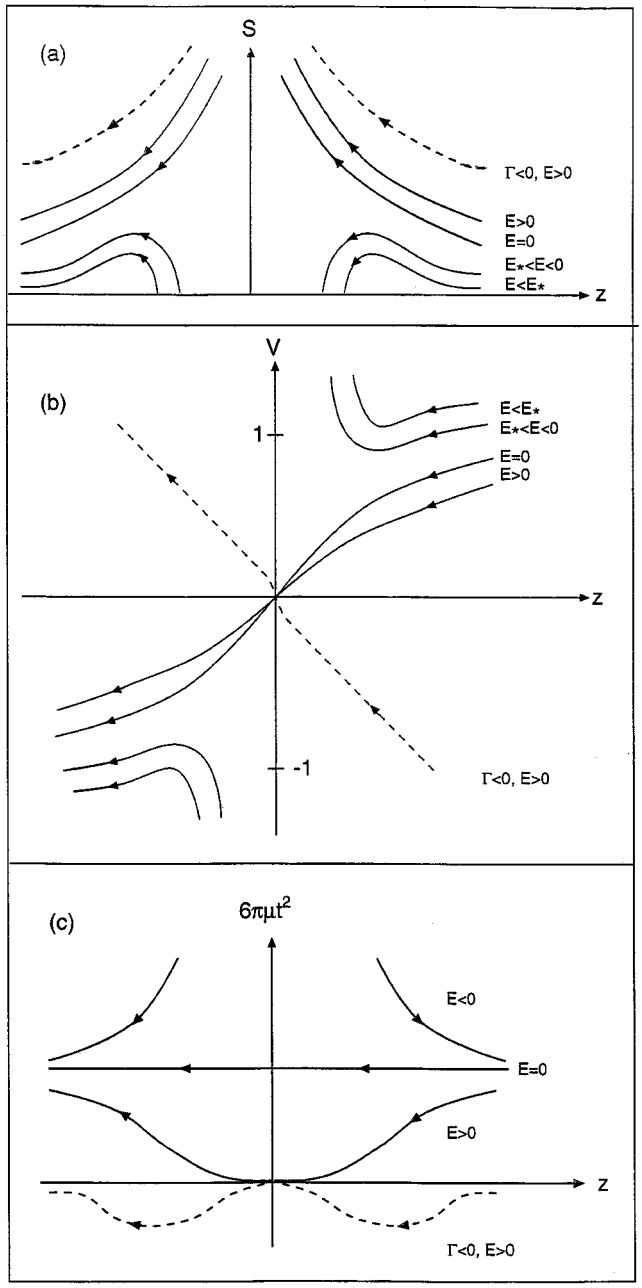

FIG. 1. This shows the form of (a) the scale factor $S(z)$, (b) the velocity function $V(z)$ and (c) the density function $\mu t^2(z)$ for the asymptotically Friedmann dust models, the arrows indicating the direction of increasing time. The solutions are described by a single parameter E, where $E=0$ in the exact Friedmann case: the $z>0$ solutions are overdense and collapse to black holes for $E<0$ (with an event horizon for $E>E_*$ since $V_{min}<1$) but they are underdense and expand forever for $E>0$. The $z<0$ solutions are just the time reverse of these. The dotted curve corresponds to a solution with negative mass; it is probably unphysical but relates to the Kantowski-Sachs solution which arises when there is pressure.

$$z_S=\frac{(-2E)^{3/2}}{2\pi\sqrt{1+2E}} \tag{3.3}$$

for $E<0$. Note that z_S corresponds to the physical origin since $R=rS=0$ there. The form of $V(z)$ in the $z>0$ solutions is shown in Fig. 1(b). In the $E\geqslant 0$ case, V decreases monotonically from ∞ to 0. In the $E<0$ case, it reaches a minimum before rising to ∞ at z_S. One can show that the values of z and V at the minimum both decrease as E increases; the minimum will exceed 1 (in which case the whole Universe is inside the black hole) if E is less than some critical negative value E_* and it will be less than 1 (in which case there is a black hole event horizon and a cosmological particle horizon) if E exceeds E_*. The solutions with $z<0$ are the time-reverse of the $z>0$ ones and the sign of V is also reversed: as t increases from $-\infty$ to 0 (i.e. as z decreases from 0 to $-\infty$), the $E\geqslant 0$ models collapse from an infinitely dispersed state ($S=\infty$) to a big crunch singularity ($S=0$); the $E<0$ models also collapse to a big crunch singularity but they emerge from a white hole and are never infinitely dispersed.

Both S and V have the same z-dependence as in the $E=0$ Friedmann solution as $|z|\to\infty$:

$$S\approx[9\sqrt{1+2E}/2]^{1/3}|z|^{-2/3},\quad V\approx[6(1+2E)]^{-1/3}z^{1/3}. \tag{3.4}$$

However, the $E\neq 0$ solutions deviate from the $E=0$ solution at small values of $|z|$. The $E<0$ solutions never reach $z=0$ at all, while the $E>0$ ones have

$$S\approx(2E)^{1/2}|z|^{-1},$$
$$V\approx-(1+2E)^{1/2}E^{-1}z\ln[(2E)^{3/2}(1+2E)^{1/2}|z|] \tag{3.5}$$

as $|z|\to 0$. The first relation implies that the circumference function $R(r,t)=Sr$ is non-zero in limit $r\to 0$ unless $E=0$ since

$$R(0,t)=\sqrt{2E}\,t. \tag{3.6}$$

This means that the ''coordinate'' origin ($r=0$) is an expanding 2-sphere. (This feature is specific to the dust case and does not arise if there is pressure.) This has a natural physical interpretation, since the forms of S and V are similar to those in the Kantowski-Sachs solution [13], in which all the matter is localized on a shell [cf. Eqs. (3.19) and (3.23) in Ref. [12]], although there is no *exact* self-similar Kantowski-Sachs solution in the dust case. To obtain a complete solution, one must therefore match the self-similar solution onto a (non-self-similar) part inside $R(t,0)$. In the $E<0$ case, we have seen that the physical origin is the black hole singularity z_S, so only for $E=0$ can one identify $z=0$ with the physical origin.

The form of the density function μt^2 can be derived from Eq. (2.33) and is shown in Fig. 1(c). For a given fluid element (i.e. fixed r), this specifies the density as a function of time $\mu(t)$. For a given time, it also specifies the density profile $\mu(r)$ and this illustrates that a non-zero value of E necessarily introduces an inhomogeneity into the model. Solutions with $E>0$ are everywhere underdense relative to the Friedmann model, with Eqs. (2.33) and (3.5) implying that μt^2 goes to 0 as $(\ln|z|)^{-1}$ as $z\to 0$. (This suggests that the interior non-self-similar region should be a vacuum.) Solu-

tions with $E<0$ are everywhere overdense relative to Friedmann, with μ diverging at the singularity. Note that Eqs. (2.33) and (3.4) imply that μt^2 is independent of E to 1st order as $|z|\rightarrow\infty$.

The form of the mass function $M(z)$ in the $D=0$ solutions is not shown explicitly but can be immediately deduced from the expression for S since Eq. (2.22) gives $M=\Gamma/S$. In the $E\geqslant 0$ case, there is always a single point where $M=1/2$ and this corresponds to the cosmological apparent horizon. In the $E<0$ case, Eq. (2.29) implies that S has a maximum of $\Gamma/|E|$ and so Eq. (2.22) shows that M has a minimum of $|E|$. Since this is less than 1/2, there are always two points where $M=1/2$, one corresponding to the black hole apparent horizon and the other to the cosmological apparent horizon. Note that a black hole's apparent horizon always lies within or coincides with its event horizon [14], which is why the first can exist without the second. Equations (2.22) and (3.3) imply that the mass associated with this singularity is

$$m_S=(MSz)_S t=(-2E)^{3/2}t/(2\pi). \tag{3.7}$$

It therefore starts off zero when the singularity first forms at $t=0$ but then grows as t. The mass of the black hole is given by a similar formula but with z having the value appropriate for the event horizon or apparent horizon. Since the former may not exist, it is more appropriate to use the latter.

Finally, we consider the $E>0$ negative-mass solutions given by Eq. (2.30). Their form is indicated by the dotted curves in Fig. 1. S, V and μ have the same form as in the positive mass solutions for small values of $|z|$ except that V and μ reverse their signs. However, the solutions are very different at large values of $|z|$ since Eq. (2.30) shows that S must always exceed $|\Gamma|/E$. Indeed it tends to this value asymptotically, so we have

$$S\approx\sqrt{1+2E}/E, \quad V\approx -z/E, \quad \mu r^2\approx -E^3/\sqrt{1+2E} \tag{3.8}$$

as $|z|\rightarrow\infty$. The form of this solution is closely related to that of the $\alpha\ll 1$ static solution [cf. Eq. (3.29) of Ref. [12]], although there is no static solution in the $\alpha=0$ case itself.

C. $E=0$ solutions

We now put $E=0$ and consider the effect of introducing a non-zero value for the constant D. [In this case, Eq. (2.28) does not permit $\Gamma<0$, so there are no negative-mass solutions.] Some of these solutions were also considered briefly by Ori and Piran [6]. The form of $S(z)$ for the $D>0$ solutions is shown in Fig. 2(a). There are two types of solutions in this case, one expanding and the other collapsing. For the expanding solutions (solid lines), $S=0$ at $z=-1/D$ and so the big bang occurs before $t=0$ (i.e. it is ''advanced''). As t increases to 0 (i.e. as z decreases to $-\infty$), S tends to the finite value

$$S_\infty(D)=(3D/\sqrt{2})^{2/3}. \tag{3.9}$$

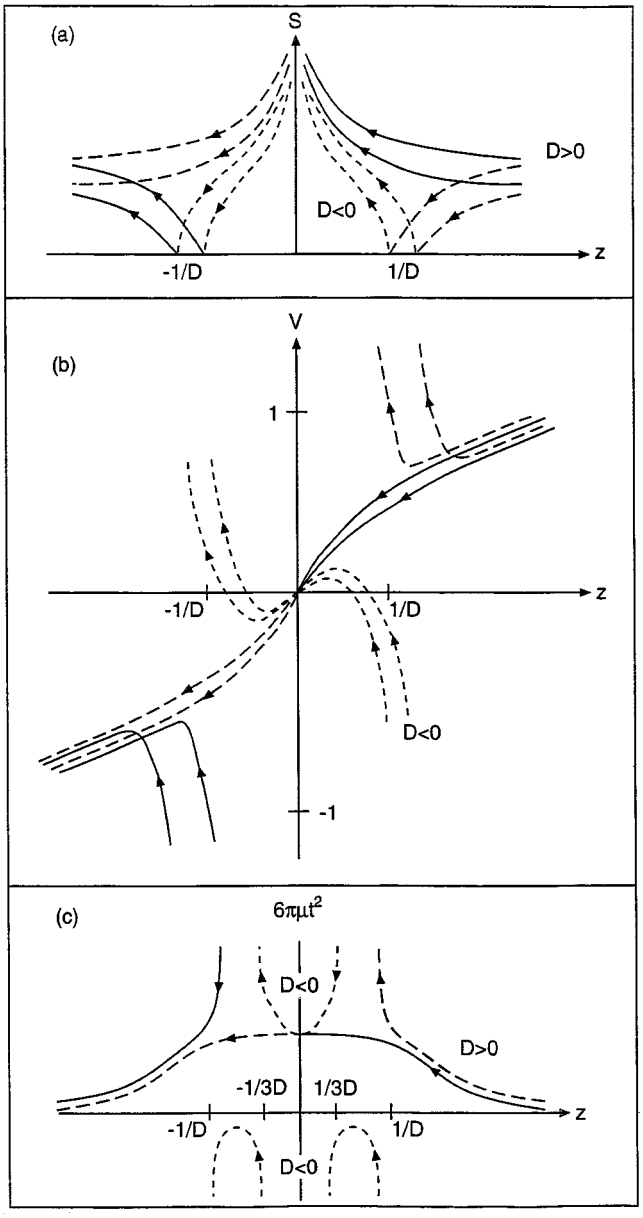

FIG. 2. This shows the form of (a) the scale factor $S(z)$, (b) the velocity function $V(z)$ and (c) the density function $\mu t^2(z)$ for dust models with $E=0$. Two different values of D are shown in (a) and (b) but only one in (c). These solutions necessarily span both positive and negative values of z. For $D>0$ they represent monotonically expanding (solid) or collapsing (broken) solutions and the latter contain a naked singularity ($V_{min}<1$) if D exceeds some value D_+ (as assumed here). The $D<0$ models (dotted) undergo shell-crossing before encountering the singularity and are probably unphysical since V and μ go negative.

As t further increases from 0 to $+\infty$ (i.e. as z jumps to $+\infty$ and then decreases to 0), S increases monotonically to ∞. For the contracting solutions (broken lines), S starts infinite at $t=-\infty$ ($z=0$) and then decreases to $S_\infty(D)$ as t increases to 0 ($z\rightarrow-\infty$). As t further increases (i.e. as z jumps to $+\infty$ and then decreases), S continues to decrease until it reaches 0 at the big crunch singularity at $z=1/D$. Both types of solutions are characterized by the fact that they have just one

singularity and span both positive and negative values of z. Note that for each value of S_∞ the two asymptotic solutions just correspond to the plus and minus signs in Eq. (2.28).

The form of $V(z)$ in the $D>0$ solutions is shown in Fig. 2(b). For the expanding solutions (solid lines), it starts off at $-\infty$ at the big bang ($z=-1/D$), reaches a negative maximum and then, from Eq. (2.31), tends to

$$V=S_\infty(D)z=(3D/\sqrt{2})^{2/3}z \tag{3.10}$$

as $z\to-\infty$. When z jumps $+\infty$, V becomes positive but Eq. (3.10) still applies. As z decreases from $+\infty$ to 0, V decreases monotonically to 0. For the contracting models (broken lines), V starts from 0 at $z=0$ and monotonically decreases as z goes to $-\infty$, being again given by Eq. (3.10) asymptotically. When z jumps to $+\infty$, V jumps to $+\infty$ and then decreases to a minimum before rising to infinity at the big crunch singularity. A simple calculation (see later) shows that the values of $|z|$ and $|V|$ at the stationary point are given by

$$|z|_{min}=\left(\frac{2+\sqrt{3}}{3D}\right),\quad |V|_{min}=\left(\frac{26+15\sqrt{3}}{3D}\right)^{1/3}, \tag{3.11}$$

so the stationary point moves towards the origin and the value of $|V|_{min}$ decreases as D increases. Note that the maximum value of V for the expanding solutions will exceed -1 and the minimum value for the contracting ones will be less than $+1$ if D exceeds some critical value $D_+=26/3+5\sqrt{3}\approx 17$. For $D>D_+$, the condition $|V|=1$ will be satisfied at *three* values of z. As illustrated by Fig. 14 of Ref. [6], this means that the contracting solutions will form a black hole in which the central singularity is naked for a while. This applies for both the solutions shown in Fig. 2(b).

The crucial feature of these solutions is that, while the form of $V(z)$ is like that in the $D=0$ case for small $|z|$, V scales as z rather than $z^{1/3}$ [cf. Eq. (3.4)] for large $|z|$. This is because any solution with finite S at infinity must be ''nearly'' static in the sense that dS/dz tends to zero. However, the solutions are not asymptotic to an *exact* static solution (indeed this does not exist in the $\alpha=0$ case) because Eq. (2.32) implies that V_R tends to a non-zero value:

$$V_R^\infty=\pm\left(\frac{4}{3D}\right)^{1/3}. \tag{3.12}$$

We therefore term these solutions asymptotically ''quasi-static.'' If V_R^∞ is positive, the fluid is collapsing at infinity; if V_R^∞ is negative, it is expanding. Note that Eq. (2.28) implies that both dS/dz and zdS/dz tend to zero at large $|z|$ but z^2dS/dz [which directly relates to V_R^∞ from Eqs. (2.28) and (2.32)] tends to a non-zero value except in the limit $D\to\infty$.

The form of the density function μt^2 in the $D>0$ solutions is also interesting and is illustrated in Fig. 3(c). From Eq. (2.33) the density parameter is given by

$$\Omega\equiv 6\pi\mu t^2=\frac{1}{(1\mp 3Dz)(1\mp Dz)} \tag{3.13}$$

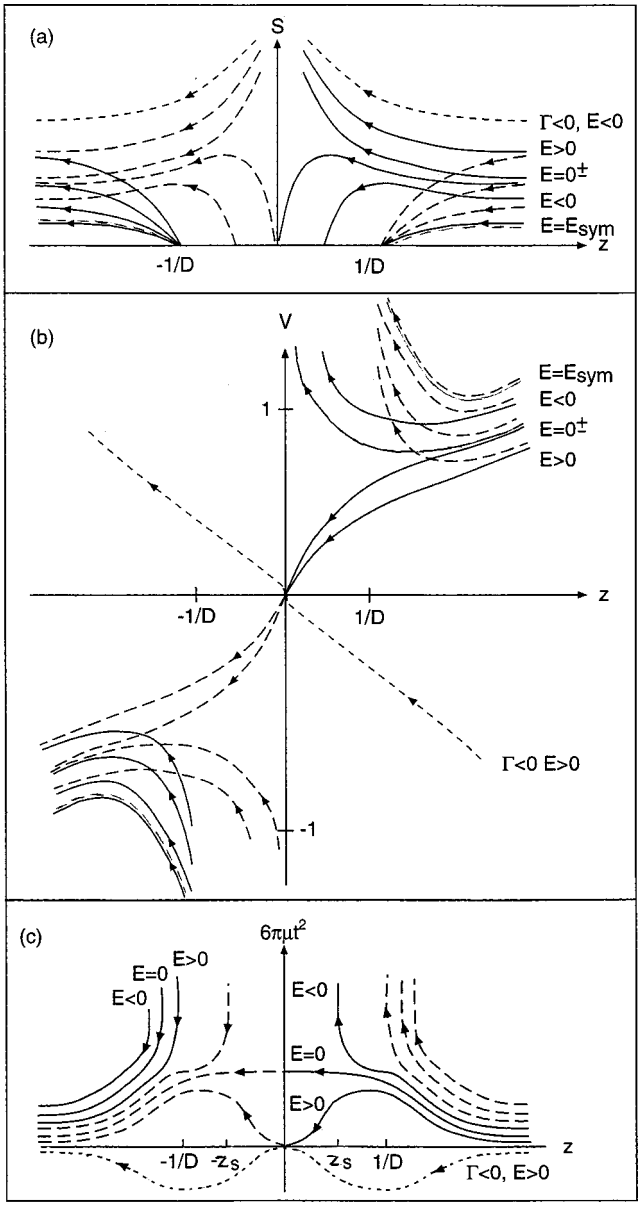

FIG. 3. This shows the form of (a) the scale factor $S(z)$, (b) the velocity function $V(z)$ and (c) the density function $\mu t^2(z)$ for the asymptotically quasi-static dust solutions. These are described by two parameters (D and E) but we assume that D is fixed and not all the solutions in (a) and (b) are shown in (c). For $E>0$ the solutions resemble those in Fig. 2, with both monotonically expanding (solid) and collapsing (broken) solutions. The collapse singularity is naked ($V_{min}<1$) if E is less than a value $E_+(D)$. For $E<0$ there are also solutions which recollapse to a black hole (solid) or emerge from a white hole (broken), as in the asymptotically Friedmann case. As E decreases, the last solution is the symmetrical one, for which $E=E_{sym}$ and $z_S=1/D$, so that the solid and broken curves coincide. The curves labelled $E=0^+$ and $E=0^-$ show the qualitative transition as E passes through 0. The dotted curves correspond to an (unphysical) negative mass solution.

where the upper and lower signs apply for positive and negative values of dS/dz, respectively. [The inverse of the factor $6\pi t^2$ corresponds to the density in a flat Friedmann dust universe, as indicated by Eq. (3.1).] For a given fluid ele-

ment, this describes how the density evolves as a function of time and it has the expected form. However, at a given time it also prescribes the density profile and one sees immediately that a non-zero value of D (like a non-zero value of E) introduces an inhomogeneity. This inhomogeneity has a particularly interesting form. In the $z<0$ regime, the profile for the collapsing solutions is homogeneous for $|z| \ll 1/D$ but has $\mu \sim r^{-2}$ for $|z| \gg 1/D$ (i.e. it resembles an isothermal sphere with a uniform core). In the $z>0$ regime, the collapsing solutions again have $\mu \sim r^{-2}$ for $|z| \gg 1/D$ but the density diverges at $z=1/D$ (i.e. one has a density singularity at the center of an isothermal sphere). For the expanding solutions, the signs of z are reversed. These features are illustrated in Fig. 2(c) and have an obvious physical interpretation.

Although the asymptotically quasi-static solutions have a natural cosmological interpretation when z is allowed to span both positive and negative values, we see that the $z>0$ and $z<0$ solutions also have a non-cosmological interpretation when considered separately: they just represent collapsing and expanding self-similar models which evolve from an initially isothermal distribution. It is interesting that the isothermal model (which is usually associated with a static solution) features prominently in both regimes, despite the fact that there is no exact static solution in the dust case.

The mass function is $M=S^{-1}$ in this case and therefore decreases or increases monotonically. There is just one value of z at which $M=1/2$ (corresponding to a black hole or cosmological apparent horizon) but this may be in either the positive or negative z region. Equation (3.9) implies that the asymptotic value of M as $|z| \to \infty$ is less than 1/2 for $D>4/3$. In this case, the collapsing solutions have their apparent horizon in $z>0$, whereas the expanding ones have it in $z<0$. The mass of the (possibly naked) singularity in these solutions is

$$m_S=(MSz)_S t=t/D \tag{3.14}$$

from Eq. (2.22). As in the asymptotically Friedmann case, it starts off zero at $t=0$ but then grows as t. In the limit $D \to \infty$, one gets a naked singularity of zero mass at the origin (cf. the static solution in the $\alpha \neq 0$ case).

Finally, we consider the $D<0$ solutions. The form of $S(z)$ in this case is shown by the dotted curves in Fig. 2(a). Such solutions are confined to $|z|<-1/D$, with S either decreasing monotonically for $z<0$ (i.e. as t increases from $-\infty$) or increasing monotonically for $z>0$ (i.e. as t increases to $+\infty$). However, these solutions break down when S is too small. This is because Eq. (2.31) implies that $|V|$ increases to some maximum value and then falls to zero at $|z|=-1/(3D)$; this is indicated by the dotted curves in Fig. 2(b). From Eq. (2.33) this means that the density diverges there, as shown by the dotted curves in Fig. 2(c). This divergence is associated with the formation of a shell-crossing singularity since the model resembles the Kantowski-Sachs solution [13] at this point. For $-1/D>|z|>-1/(3D)$, the density and velocity functions become negative but this is presumably unphysical.

D. $D \neq 0, E \neq 0$ solutions

The forms of $S(z)$ for the $(D>0, E \neq 0)$ solutions are indicated in Fig. 3(a). The figure assumes that D is fixed but allows E to vary. The $(D>0, E>0)$ solutions are qualitatively similar to the $(D>0, E=0)$ ones in that they are monotonically expanding or collapsing and span both positive and negative z, as illustrated by the upper solid and broken curves, respectively. They are also asymptotically quasi-static, in the sense that S tends to a finite value as $|z| \to \infty$, even though V_R is non-zero there from Eq. (2.32). The form of the solutions near $z=0$ is still given by Eqs. (3.5) for $E>0$, so the behavior is like that in the $(E>0, D=0)$ case here. In particular, $z=0$ no longer corresponds to the physical origin, so one again has to attach the solution to a non-self-similar central region.

The $(D>0, E<0)$ solutions are qualitatively different from the $(D>0, E=0)$ ones in that the models no longer collapse from or expand to infinity. This is clear from Eq. (2.28), which implies that S has a maximum value of $\Gamma/|E|$, so all the solutions start off expanding and then recollapse. Note that there is no exact static solution since that would be incompatible with Eq. (2.13), the term on the right-hand side being non-zero for $\alpha=0$. Figure 3(a) shows that there are two types of $(D>0, E<0)$ solutions. One type (illustrated by the lower solid curves) expands from the big bang singularity at $z=-1/D$ and then recollapses to a black hole singularity at

$$z_S=\left[\frac{2\pi\sqrt{1+2E}}{(-2E)^{3/2}}-D\right]^{-1}. \tag{3.15}$$

This reduces to the value given by Eq. (3.3) if $D=0$. The other type (illustrated by the lower broken curves) expands from a white hole singularity at $-z_S$ and then recollapses to a big crunch singularity at $z=1/D$.

Equation (3.15) implies that $z_S=1/D$, so that the solution is symmetric in z, if D has the value

$$D_{sym} \equiv \frac{\pi\sqrt{1+2E}}{(-2E)^{3/2}}. \tag{3.16}$$

One can invert this condition to obtain the associated value of E in terms of D:

$$E_{sym} \equiv -\frac{4\pi}{\sqrt{3}D}\sinh\left[\frac{1}{3}\sinh^{-1}\left(\frac{3\sqrt{3}D}{8\pi}\right)\right] \tag{3.17}$$

and this specifies a 1-parameter family of solutions with $V_R^\infty=0$. If one considers the limit of the symmetric solution as $D \to 0$, one finds $E_{sym} \to -1/2$ and $z_S \to \infty$. On the other hand, if one considers the limit as $D \to \infty$, one finds $E_{sym} \to 0$ and $z_S \to 0$, so that both singularities go the origin. This is the closest one can get to a static solution in the dust case. Note also that $z_S \to 0$ in the limit $E \to 0^-$ whatever the value of D; the sudden transition as one goes from $E=0^-$ to $E=0^+$ is illustrated in Fig. 3(a).

This value of E given by Eq. (3.17) has a special physical significance in that it prescribes the *minimum* value of E

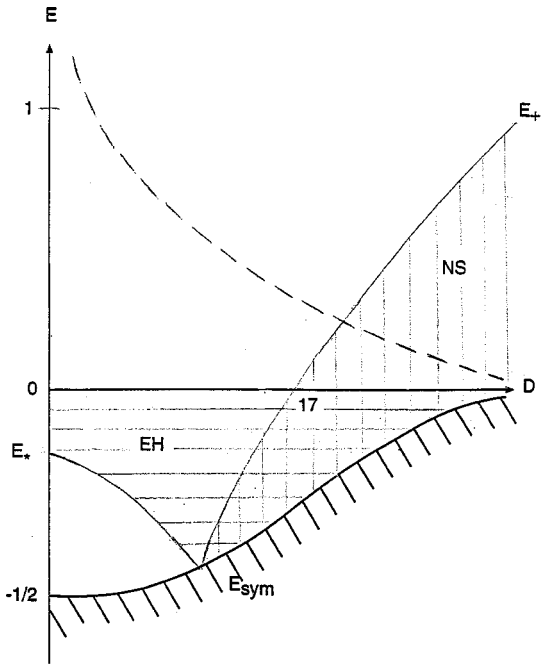

FIG. 4. This shows the permitted regime for the parameters E and D. The curve labelled E_{sym} indicates the symmetric solution and all physical solutions must lie above this. The upper broken line gives the transition between different asymptotic forms for S_∞ and V_∞. The collapsing solutions have a naked singularity in the vertically shaded region below the line labelled E_+ and the black hole solutions have an event horizon and a particle horizon in the horizontally shaded region above the line labelled E_*. These lines intersect on the lower boundary.

allowed for given D, as indicated by the lower boundary in Fig. 4. The proof of this is as follows. If one takes the limit of Eqs. (2.14) and (2.15) with $\alpha=0$ as $z\to\infty$, using Eqs. (2.19) and (2.32) and the fact that $\dot{S}\to 0$ from Eq. (2.28), one obtains

$$z^2\dot{S}^2=(1+2E)(V_R^\infty)^2=(4\pi\mu r^2)_\infty^2 S_\infty^6+(8\pi\mu r^2)_\infty S_\infty^2-1 \tag{3.18}$$

where one can regard $(\mu r^2)_\infty$ and S_∞ as independent asymptotic parameters. If one now fixes $(\mu r^2)_\infty$ and assumes that it is positive, then the right-hand side of Eq. (3.18) decreases monotonically with decreasing S_∞. One therefore gets a *real* solution for V_R^∞ only if S_∞ exceeds a certain value and—by monotonicity—this must be the value associated with the symmetric solution. Thus a real solution (with positive density) exists only for $E>E_{sym}$ or, equivalently, $D<D_{sym}$. This means that z_S is always positive and less than $1/D$ and that the maximum of S will always occur at the opposite sign of z as the $|z|=1/D$ singularity. These features are illustrated by the curves in Fig. 3(a).

The form of $V(z)$ in these solutions is shown in Fig. 3(b). For $(D>0,E>0)$ it is similar to that in the $(D>0,E=0)$ case. As z decreases from 0 to $-\infty$, V decreases monotonically from 0 to $-\infty$ for the collapsing solutions; it then jumps to $z=+\infty$ and, as z continues to decrease, it falls to a minimum and rises to infinity at the big crunch singularity at $z=1/D$. Also as in the $(D>0,E=0)$ case, this minimum will fall below 1, corresponding to a naked singularity, providing D exceeds some value $D_+(E)$. We derive an implicit expression for $D_+(E)$ later but, for the present, note that it increases with increasing E and reduces to the value D_+ which arose in Sec. III C when $E=0$. The condition for a naked singularity can also be expressed as the requirement that E be less than some critical value $E_+(D)$.

For $(D>0,E<0)$ the form of V is similar to that in the $(D=0,E<0)$ case, except that the curves are no longer symmetric. As z decreases from $-1/D$, V rises from $-\infty$ until some maximum for the first type of solution and then falls to $-\infty$ quasi-statically as $z\to-\infty$. It then jumps to $z=+\infty$ and falls to a minimum before rising to ∞ at z_S. As in the $(D=0,E>0)$ case, there will be a black hole event horizon if the minimum value of V is less than 1; this requires that E exceed some value $E_*(D)$, which must reduce to the value E_* given in Sec. III B when $D=0$. We derive an implicit expression for $E_*(D)$ below. It should be stressed that the value $E_*(D)$ is associated with the minimum of $|V|$ near the singularity at $|z|=z_S$ and is different from the value $E_+(D)$ associated with the minimum near $|z|=1/D$. The relationship between the values $E_+(D)$ and $E_*(D)$ is discussed below.

In order to understand the form of the curves in Figs. 3(a) and 3(b) more precisely, it is useful to specify their asymptotic behavior. As $|z|\to\infty$, Eqs. (2.29) and (2.31) with $E>0$ imply that $S(z)$ and $V(z)$ have the following asymptotic forms:

$$S_\infty\approx D\sqrt{2E},\quad V_\infty\approx\left(\frac{2E}{1+2E}\right)^{1/2}Dz \tag{3.19}$$

for $D\gg[(1+2E)/E^3]^{1/2}$ and

$$S_\infty\approx\left(\frac{1+2E}{4}\right)^{1/6}(3D)^{2/3},\quad V_\infty\approx\frac{(3D)^{2/3}z}{2^{1/3}(1+2E)^{1/3}} \tag{3.20}$$

for $D\ll[(1+2E)/E^3]^{1/2}$. The transition value for D between these two regimes is just an extrapolation of the expression for D_{sym} given by Eq. (3.16) into the $E>0$ regime; it scales as E^{-1} for $E\gg1$ and $E^{-3/2}$ for $E\ll1$. Note that Eq. (3.20) agrees with Eqs. (3.9) and (3.10) in the limit $E=0$. For $E<0$, Eq. (3.20) still applies if $D\ll D_{sym}$ but one has

$$S_\infty\approx\sqrt{1+2E}/|E|,\quad V_\infty\approx z/|E| \tag{3.21}$$

for $D\approx D_{sym}$ (i.e. S_∞ tends to the value associated with the symmetric solution).

These equations prescribe the asymptotic forms for S_∞ and V_∞ in the different (E,D) regimes of Fig. 4. For fixed D, Eqs. (3.19) to (3.21) show that S_∞ always increases with E but is roughly constant for $|E|\ll1$. This feature is illustrated in Fig. 3(a). The behavior of V_∞ is more complicated. For $D\ll1$, it decreases with increasing E but eventually flattens off; this is the case shown in Fig. 3(b). For $D\gg1$, it is constant and then increases with E before flattening off. Note that all these solutions are quasi-static and not exactly static asymptotically since Eq. (2.32) gives

$$V_R^{\infty} \approx \pm \frac{4^{1/3}}{(3D)^{1/3}(1+2E)^{1/3}}, \quad V_R^{\infty} = \pm \left(\frac{2|E|}{1+2E} \right)^{1/2} \tag{3.22}$$

for $D \gg [(1+2E)/E^3]^{1/2}$ and $D \ll [(1+2E)/|E|^3]^{1/2}$ respectively. The sign is positive for collapsing solutions and negative for expanding ones. Note that the first expression agrees with Eq. (3.12) in the limit $E=0$.

We now derive implicit expressions for the functions $E_*(D)$ and $E_+(D)$, which are related to the existence of event horizons or naked singularities. Differentiating Eq. (2.31) shows that when $dV/dz=0$ one always has

$$V = 1/(S^2 z) \tag{3.23}$$

and Eq. (2.31) then gives

$$V\Gamma - 1/(VS) = \pm \sqrt{2E + 2\Gamma/S}, \tag{3.24}$$

where the positive and minus signs corresponds to the sign of dS/dz. If one also requires $|V|=1$ at the stationary point, Eq. (3.24) gives two roots

$$S = 2\Gamma \pm \sqrt{4\Gamma^2 - 1}, \quad |z| = 8\Gamma^2 - 1 \mp 4\Gamma \sqrt{4\Gamma^2 - 1}, \tag{3.25}$$

where the plus and minus signs are distinct from the ones appearing in Eq. (3.24). These roots can be real providing $\Gamma > 1/2$, corresponding to $E > -3/8$. However, one needs to check whether both of these solutions satisfy condition (3.24).

Inserting the solutions (3.25) into Eq. (2.29) gives an expression for D in terms of E. This expression is complicated in general but it simplifies in certain regimes. For $E \gg 1$, which implies $\Gamma \approx \sqrt{2E} \gg 1$, one obtains two possible solutions:

$$S \approx 4\Gamma, \quad |z| \approx 1/(16\Gamma^2), \quad D \approx 32E \tag{3.26}$$

and

$$S \approx 1/(4\Gamma), \quad |z| \approx 16\Gamma^2, \quad D \approx \frac{1}{E}\left(\frac{13}{32} - \ln\sqrt{2} \right) \approx 0.06E^{-1}. \tag{3.27}$$

The first has $\Gamma > 1/S$ and therefore requires $dS/dz > 0$ from Eq. (3.24), which leads to a consistent solution. However, the second has $\Gamma < 1/S$ and requires $dS/dz < 0$, which does not. In the limit $E \to 0$, which implies $\Gamma \approx 1$, one obtains

$$S \approx (2 \pm \sqrt{3})(1 \pm 2E/\sqrt{3}), \quad |z| \approx (7 \mp 4\sqrt{3})(1 \mp 4E/\sqrt{3}). \tag{3.28}$$

The upper sign gives $\Gamma > 1/S$ and therefore requires $dS/dz > 0$, which leads to a consistent solution as E tends to 0 from either above or below. Equation (2.29) then gives

$$D \approx \left(\frac{26 + 15\sqrt{3}}{3} \right) + E\left(\frac{109 + 63\sqrt{3}}{6} \right) \approx 17 + 36E. \tag{3.29}$$

Note that the constant part of this expression gives the same limiting value of D as implied by Eq. (3.11). The lower sign in Eq. (3.28) gives $\Gamma < 1/S$ and requires $dS/dz < 0$, which does not lead to a consistent solution. Finally we note that Eqs. (3.25) and (2.29) lead to unique values of E and D for which the symmetric solution has $V_{min}=1$; this necessarily corresponds to a point on the lower boundary in Fig. 4.

These limiting behaviors allow one to infer the rough form of the functions $E_*(D)$ and $E_+(D)$, as indicated in Fig. 4. Here we have used the fact that dE_+/dD is positive as $E \to 0$, as follows from Eq. (3.29). The form of the functions in the $E<0$ regime can be inferred from the fact that $E_*(D)$ must reach the value E_* mentioned in Sec. III B when $D=0$ (although this value has not been calculated explicitly). Also $E_*(D)$ and $E_+(D)$ must reach the line $E = E_{sym}(D)$ at the same value of E and this must clearly exceed $-3/8$ from Eq. (3.25). We note that, for sufficiently large values of D, there may be *both* an event horizon and a naked singularity.

The form of μt^2 in these solutions is shown in Fig. 3(c), although this gives only some of the solutions shown in Figs. 3(a) and 3(b). It can be understood as a composite of the curves shown in Fig. 1(c) for $E<0$ and Fig. 2(c) for $E>0$. From Eqs. (2.33) and (3.19) to (3.21), the asymptotic form of the density profile density is given by

$$4\pi\mu r^2 \approx \left[\frac{\sqrt{1+2E}}{D^3(2E)^{3/2}}, \quad \frac{2}{9D^2} \right] \tag{3.30}$$

for $D \gg [(1+2E)/E^3]^{1/2}$ and $D \ll [(1+2E)/|E|^3]^{1/2}$ [cf. Eq. (3.13).] The $E>0$ solutions are everywhere underdense relative to the $E=0$ solutions, going to 0 as $(\ln|z|)^{-1}$ at the origin, whereas the $E<0$ solutions are everywhere overdense and have a second density singularity. There is a uniform core region only in the $E=0$ case, although this also applies for $E<0$ if there is pressure [12].

The form of $M(z) = \Gamma/S(z)$ can be deduced immediately from Fig. 3(a). In the $E>0$ case it rises or falls monotonically, as in the $D=0$ case, so there is just one value of z for which $M=1/2$. As $|z| \to \infty$, M tends to a limiting value

$$M_\infty = \frac{\sqrt{1+2E}}{S_\infty(D,E)} \tag{3.31}$$

and the apparent horizon will be in $z>0$ or $z<0$ according to whether this is greater or less than 1/2. In the $E<0$ case, M will have a minimum where S has a maximum. This occurs at

$$|z| = \left[\frac{\pi\sqrt{1+2E}}{(-2E)^{3/2}} - D \right]^{-1} \tag{3.32}$$

and, since the minimum value is $|E|$, this is necessarily less than 1/2. One therefore has at least two points where $M = 1/2$, one of which is the apparent horizon for the black hole associated with the singularity at z_S. Therefore, as in the $D=0$ case, there will always be a black hole apparent hori-

zon but not necessarily an event horizon. This emphasizes an important difference between the collapse singularities at $z=1/D$ and $z=z_S$: only the latter is associated with an apparent horizon, which is why only the former can be naked.

The $D<0$ solutions have the same form as in the $E=0$ case, except that the $E<0$ ones have a second singularity at the value z_S given by Eq. (3.15) with $D<0$. In this case, as z goes from $-1/D$ to z_S, S first increases to some maximum value and then decreases, while V monotonically increases from $-\infty$ to $+\infty$. As in the $E=0$ case, such models are probably physically unrealistic since the density diverges due to shell crossing. They are therefore not shown explicitly. The form of the (unphysical) negative-mass solutions, which only exist for $E>0$, is indicated by the dotted curve in Fig. 3. This is similar to the $E=0$ case shown in Fig. 2 except that asymptotically Eq. (3.19) applies rather than Eq. (3.8).

IV. CONCLUSION

We may briefly summarize the results of our analysis as follows. (1) There are two families of spherically symmetric self-similar dust models: asymptotically flat Friedmann solutions and what we have termed asymptotically quasi-static solutions. These all represent inhomogeneous cosmological models in which the energy function E is constant. They either expand from a big bang or collapse to a big crunch but the singularity is only at $t=0$ for the asymptotically Friedmann family. (2) Some of the asymptotically Friedmann models represent overdensities in a Friedmann background which recollapse to a second singularity and contain a black hole which grows as fast as the Universe. The black hole always has an apparent horizon but not necessarily an event horizon. Other asymptotically Friedmann models represent underdensities in a Friedmann background which grow as fast as the Universe. (3) The asymptotically quasi-static models can be interpreted as representing inhomogenenous cosmological solutions (with one or two singularities) if one allows both signs of z, with a uniform density core in one regime and a central black hole or naked singularity in the other. If one confines attention to solutions with just one sign of z, these represent self-similar collapse from an initially isothermal distibution or the time reverse of this. (4) We have emphasized the relationship between the $z>0$ and $z<0$ solutions. Any particular asymptotically Friedmann solution is confined to one sign of z but any asymptotically quasi-static solution necessarily spans both signs.

In an accompanying paper [12] it is shown that the spherically symmetric self-similar solutions with pressure share many of the qualitative features of the dust ones, especially in the supersonic regime. In particular, all of the properties (1) to (4) above still pertain. However, it should be emphasized that new types of solution arise when there is pressure. For example, there is an exact static solution and an exact Kantowski-Sachs solution, as well as families of solutions asymptotic to these. There are also asymptotically Minkowski solutions for $\alpha>1/5$, some of which asymptote to a finite value of z. The inclusion of pressure obviously introduces qualitatively new features in the subsonic regime, in particular the possible presence of a sonic point.

In claiming that our classification is ''complete,'' it should be emphasized that our considerations have been confined to similarity solutions of the simplest kind (i.e. homothetic solutions in which the similarity variable is $z\equiv r/t$). However, it should be noted that this is not the only type of similarity. For example, Carter and Henriksen [15] have generalized the concept to include what they term ''kinematic'' self-similarity. In this context the similarity variable is of the form $z=r/t^a$ for $a\neq 1$ and the solution may contain some dimensional constant. Ponce de Leon [16] has also introduced the closely related notion of ''partial homothety.'' It is not yet clear how easily the analysis of this paper can be extended to these cases. Finally it should also be emphasized that we have only been studying solutions which are homothetic *everywhere*. The sort of models considered by Tomita [10] in which one patches a self-similar transition region between other non-self-similar regions, is clearly not covered here.

ACKNOWLEDGMENTS

The author thanks Alan Coley for useful discussions and is grateful to the Yukawa Institute for Theoretical Physics at Kyoto University and the Department of Mathematics and Statistics at Dalhousie University for hospitality received during this work.

[1] M. E. Cahill and A. H. Taub, Commun. Math. Phys. **21**, 1 (1971).
[2] R. C. Tolman, Proc. Natl. Acad. Sci. USA **20**, 169 (1934); H. Bondi, Mon. Not. R. Astron. Soc. **107**, 410 (1947); W. B. Bonnor, Astrophys. J. **39**, 143 (1956).
[3] V. T. Gurovich, Dokl. Akad. Nauk (SSR) **169**, 62 (1967) [Sov. Phys. Dokl. **11**, 569 (1967)]; C. C. Dyer, Mon. Not. R. Astron. Soc. **189**, 189 (1979); Z. C. Wu, Gen. Relativ. Gravit. **13**, 625 (1098); S. D. Maharaj, J. Math. Phys. **29**, 1443 (1988); R. N. Henriksen and K. Patel, Phys. Rev. D **42**, 1068 (1991); A. M. Sintes, Ph.D. thesis, University of Balearic Islands, 1996.
[4] B. J. Carr and S. W. Hawking, Mon. Not. R. Astron. Soc. **168**, 399 (1974).
[5] B. J. Carr and A. Yahil, Astrophys. J. **360**, 330 (1990).
[6] A. Ori and T. Piran, Phys. Rev. D **42**, 1068 (1990).
[7] A. Krasinzki, *Physics in an Inhomogeneous Universe* (Cambridge University Press, Cambridge, England, 1997).
[8] B. J. Carr and A. A. Coley, Class. Quantum Grav. **16**, R31 (1999).
[9] D. M. Eardley and L. Smarr, Phys. Rev. D **19**, 2239 (1979); D. Christodoulou, Commun. Math. Phys. **93**, 171 (1984); K. Lake, Phys. Rev. Lett. **68**, 3129 (1982); P. S. Joshi and I. H. Dwivedi, Phys. Rev. D **47**, 5357 (1993); P. S. Joshi and T. P. Singh, *ibid.* **51**, 6778 (1995); I. H. Dwivedi and P. S. Joshi, Class. Quantum Grav. **47**, 5357 (1997).
[10] K. Tomita, Astrophys. J. **451**, 1 (1995); Phys. Rev. D **56**, 3341

(1997); Gen. Relativ. Gravit. **13**, 625 (1997).
[11] B. J. Carr and A. Whinnett, report, 1999.
[12] B. J. Carr and A. A. Coley, following paper, Phys. Rev. D. **62**, 044023 (2000).
[13] R. Kantowski and R. Sachs, J. Math. Phys. **7**, 443 (1966).
[14] S. W. Hawking and G. F. R. Ellis, *The Large-Scale Structure of Spacetime* (Cambridge University Press, Cambridge, England, 1973).
[15] B. Carter and R. N. Henriksen, Ann. Phys. Supp. **14**, 47 (1989).
[16] J. Ponce de Leon, Gen. Relativ. Gravit. **25**, 865 (1993).